Chapter 9

Evaluating Cyclic Fatigue of Sealants During Outdoor Testing

R. Sam Williams,[1] Steve Lacher,[1] Corey Halpin,[1] and Christopher White[2]

[1] U.S. Department of Agriculture, Forest Service, Forest Products Laboratory, Madison, WI
[2] National Institute of Standards and Technology, Gaithersburg, MD

A computer-controlled test apparatus (CCTA) and other instrumentation for subjecting sealant specimens to cyclic fatigue during outdoor exposure was developed. The CCTA enables us to use weather-induced conditions to cyclic fatigue specimens and to conduct controlled tests in-situ during the outdoor exposure. Thermally induced dimensional changes of an aluminum bar were fed to a computer that enhanced the movement, set limits on the movement, and supplied movement information to the test apparatus. As specimens moved, load/deformation and weather conditions (temperature, relative humidity, UV radiation, precipitation, and wind velocity) were measured every few minutes to give an extensive database containing these variables. In addition, controlled tests were done every four hours during the exposure. At these four-hour intervals, the computer was programmed to interrupt weather-induced cyclic fatigue and conduct a standard-strain test. The data enabled us to calculate the elastic modulus of each specimen at any time during the exposure and to construct a model that fit the observed temperature and relative humidity effects on modulus.

INTRODUCTION

Background

Sealants (caulking compounds) are used extensively in the outdoor envelope of residential construction to seal against water intrusion. They often fail shortly after installation because of improper joint design, incompatibility with the substrate, poor application practices, and excessive movement of wood and wood-based materials.

As part of ongoing work on materials used in residential construction, studies on sealants began in 2002 at the USDA Forest Service, Forest Products Laboratory, Madison, WI, in cooperation with the National Institute of Standards and Technology (NIST) in Gaithersburg, MD, and several sealant manufacturers. These studies resulted in several publications that described the construction of test apparatuses, instrumentation of indoor and outdoor test facilities, data collection systems, and data analysis methods.[1-8] This work involved detailed laboratory and field studies designed to develop service life prediction methods for sealants. Studies are continuing, and a critical part of the work is the measurement of load and deflection of specimens as they are fatigue-cycled during outdoor exposure. Measurements can be combined with measurements of the environmental "dose" (various weather factors that may cause a load/deflection or degradation) to form a dose-response relationship that expresses degradation of specimens as a function of exposure conditions rather than exposure time. The dose-response of the sealant obtained from outdoor testing accomplishes several advances over traditional time-response experiments. The critical factors causing degradation can be established, interactions among factors can be determined, and dose-response from outdoor experiments can be compared with dose-response from accelerated laboratory experiments to obtain a meaningful acceleration factor.

The overall objective of our studies was to develop a protocol for predicting the service life of sealant formulations and to identify the fundamental mechanism of early failure. This protocol included both accelerated laboratory and outdoor exposures. All outdoor weathering factors—temperature, ultraviolet (UV) radiation, relative humidity (RH), wind velocity, and rainfall—and their amount (dose) were monitored, and the sealant degradation (material response) was linked to the dose. In short, our objectives were to (1) gather real-time data of stress and strain of sealants during outdoor exposure, (2) gather real-time data on weather, including UV radiation, and (3) match sealant response to accumulated environmental stresses. Ultimately, our goal is to use the information from outdoor materials response and weather data to develop appropriate accelerated tests and the capability to determine service life in less than real time with statistical confidence and reasonable accuracy.

Weather and Weathering Factors

Weathering factors are solar radiation, abrasion, pollutants, changes in temperature and relative humidity, and wet/dry and freeze/thaw cycles. The weather at any location can be quite variable from day to day and year to year. For example, the record high in Madison, WI, on June 21, was 100°F (38°C) in 1988; the record low was 36°F (2°C) in 1992. The average high/low temperature on June 21 is 80°/57°F (27°/14°C). The average temperature is rather meaningless in terms of the material degradation if the actual temperature can vary over such a wide range. Many materials, particularly polymeric, may be at a different state (above or below the glass transition), which could greatly influence the rate and mechanism of degradation. Average

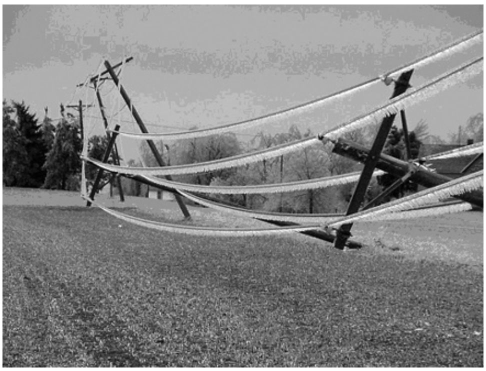

Figure 1—Severe weather and damage resulting from freezing rain (courtesy of John Walker, Boone REMC, Lebanon, IN).

weather is comprised of large variation and often includes severe weather conditions (*Figure* 1).

In reviewing the work in our laboratory and similar work reported by others who have developed accelerated test methods, two problems became obvious. First, weather is not consistent from day to day, season to season, year to year, and century to century.[9] Second, weather data have not been used in any meaningful way during outdoor exposure. That is, there has been no link between specific weather events and the response of materials to these events. Thus, a variety of weathering events that may have had a dramatic influence on degradation have only been averaged. There has been no way of knowing what the conditions were when the specimens degraded. The specimens may have degraded more or less at the same rate since the previous evaluation, or all of the degradation could have occurred during a single weather event, such as freezing rain (*Figure* 1). Periodic evaluations—the standard method used in accelerated tests—show only the change since the previous evaluation, not the conditions that caused the change. Results have often been misleading because critical factors causing the degradation were either not known or not measured.

Reliability-Based Service Life Prediction

Reliability-based service life prediction depends on accurate and precise measurement of specimen response as it degrades, measurement of degrading factors, and integration of the factors to obtain the dose. Field data can then be compared with accelerated laboratory tests using dose and response rather than some response versus time (*Figure* 2).

Traditional methods for linking outdoor weathering tests with accelerated laboratory tests usually involve a weathering device programmed with a wet/dry and UV radiation cycle to approximate the outdoor weather. UV radiation from a carbon arc[10] was used in early weathering devices; to a great extent, this source was later replaced by a xenon-arc source.[11,12] Other devices use UV fluorescence light sources.[13,14] Considerable effort has been made to develop a light source that duplicates natural sunlight. Researchers continue to search for the correct cycle that replicates outdoor conditions. Researchers want accelerated tests that predict the degradation that occurs in actual use, but it is difficult to ensure that the degradation mechanism is the same in the test and in actual use. If the mechanism of degradation is not the same, there is little chance that the accelerated test will give reliable results. The key to ensuring that the degradation mechanism is the same in various exposure conditions is to monitor the chemical changes. Other than recent work by Martin and others at the National Institute of Standards and Technology (NIST), few

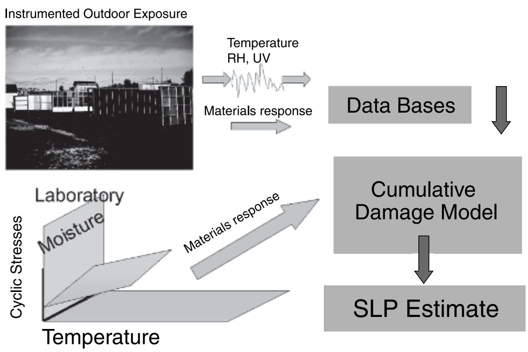

Figure 2—Reliability-based service life prediction (SLP) methodology.

attempts have been made to measure chemical changes occurring in materials exposed outdoors and link them to chemical changes in materials exposed in accelerated laboratory tests.[15-17]

Previous Sealant Tests

Sealants (caulking compounds) have become widely used in commercial and residential structures to help seal their exterior envelope against water intrusion. Sealants are formulated to accommodate cyclic stress and strain, but they may undergo cyclic fatigue in combination with other degrading factors.

General guidelines for accelerated testing of sealants are described by ASTM C 1442, Standard Practice for Conducting Tests on Sealants using Artificial Weathering Apparatus.[18] Other ASTM methods for accelerated weathering of sealants are C 718–93 (UV–Cold Box Exposure of One-Part, Elastomeric, Solvent-Release Type Sealants), C 732–95 (Aging Effects of Artificial Weathering on Latex Sealants), C 734–93 (Low-Temperature Flexibility of Latex Sealants After Artificial Weathering), C 793–97 (Effects of Accelerated Weathering on Elastomeric Joint Sealants), C 1257 (Accelerated Weathering of Solvent-Release-Type Sealants), and D 2249 (Predicting Effect of Weathering on Face Glazing and Bedding Compounds on Metal Sash).[19-24] These tests use a weathering device with UV radiation and intermittent water spray to accelerate degradation. The tests are not meant to predict the exact service life nor the mechanism of failures, but are more qualitative evaluations of sealant performance.

The Hockman Cycle, a standard that combines cyclic stress (fatigue), water immersion, and temperature change, was initially developed by A. Hockman at NIST.[25] Several devices have been used to induce cyclic movement (fatigue) of sealants during exposure. These devices generally use thermally induced dimensional change to cause fatigue in a sealant. For example, Onuoha[26] used unplasticized polyvinyl chloride (PVC) pipe to produce fatigue in one-part polyurethane and polyurethane-hybrid sealants. Racks have also been built using dissimilar materials such as wood and aluminum,[27] concrete and aluminum,[28] and steel and aluminum[29,30] to develop fatigue stresses. Manually operated devices have been used to create cycling effects.[31-33] Lacasse and Margeson[34] cycled sealants during cure. Bolte et al.[35] reported on cyclic movement of sealants during cure in natural and artificial weathering. Liu and Wang[36] used cyclic freeze-thaw cycles to test sealants used for horizontal joints in concrete. Al-Qadi et al.[37,38] also evaluated sealants used for concrete slabs using cyclic shear and static horizontal deflection. Using the RILEM TC139-DBS test method, Miyauchi et al.[39] conducted durability

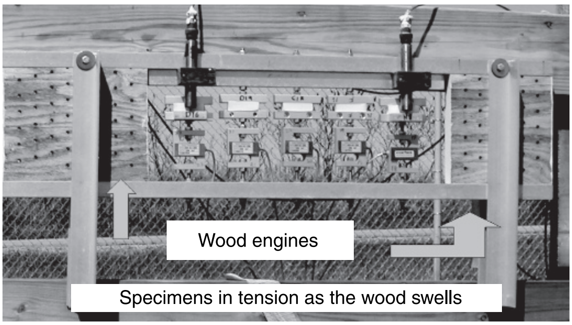

Figure 3—Sealant specimens attached to wood-driven TS cyclic test apparatus: the apparatus places the specimens in tension (T) as the wood swells (S).

tests that included cyclic fatigue in combination with exposure to UV radiation in a xenon-arc weathering device. Sharman et al.[40] evaluated sealants in outdoor exposure using a cyclic movement test apparatus. Koike et al.[41] cycled sealants in laboratory tests at temperatures of 0–80°C and calculated modulus and loss tangent. Marechal and Kalifa[42] used cyclic movement during artificial weathering to evaluate sealant performance under three different simulated climate conditions. Beech[43] reviewed test methods for sealants. Wolf [44,45] reviewed the correlation of long-term artificial aging and outdoor exposure of sealants. Wolf and Seneffe[46] reported on work within ISO TC 59/SC8 and RILEM TC139-DBS committees since 1990 that dealt with developing meaningful tests for sealants. In previous reports describing sealant tests, environmental factors were not recorded in an ongoing basis. Therefore, it was not possible to correlate the dose of degrading factors with quantifiable changes in chemical or physical properties. Evaluations were usually done on a predetermined schedule (weekly, monthly, or biannually) and involved only a visual examination. This examination might indicate an adhesive or cohesive failure, but it was impossible to determine when the specimens failed or the conditions that caused the failure.

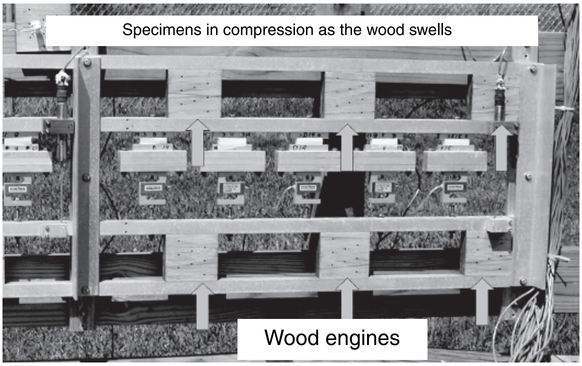

Figure 4—Sealant specimens attached to wood-driven CS cyclic test apparatus: the apparatus places the specimens in compression (C) as the wood swells (S).

Wood-Based Cyclic Fatigue Apparatus

In our previous cyclic fatigue studies,[5–7] the weather-induced movement of sealant specimens was obtained from the dimensional change in flat-sawn (tangential) blocks of red oak (*Quercus rubra*). Precipitation and/or changes in relative humidity caused the wood to change moisture content, thus giving the required dimensional change. Two designs (TS and CS) were developed for conducting these exposure tests. In TS (*Figure* 3), the test specimens are placed in tension (T) by an increase in moisture content of the wood (as the wood swells [S]). This subjects the

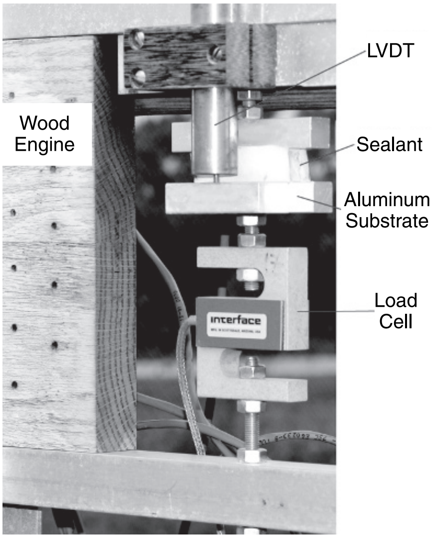

Figure 5—Close-up of specimens on the wood driven test apparatus showing the specimen, load cell, and the linear variable differential transformer (LVDT).

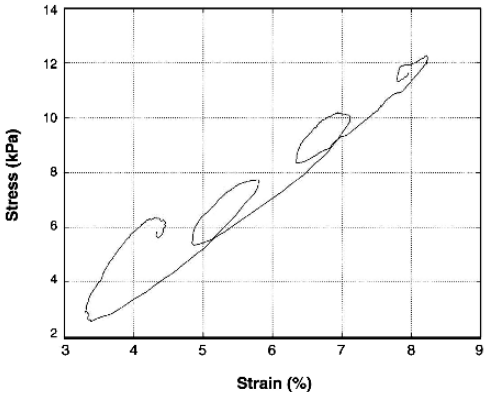

Figure 6—Stress-strain plot of a sealant specimen showing diurnal cycles and superimposed on an overall decrease in tension over four days. The beginning of the four-day period is at the top.

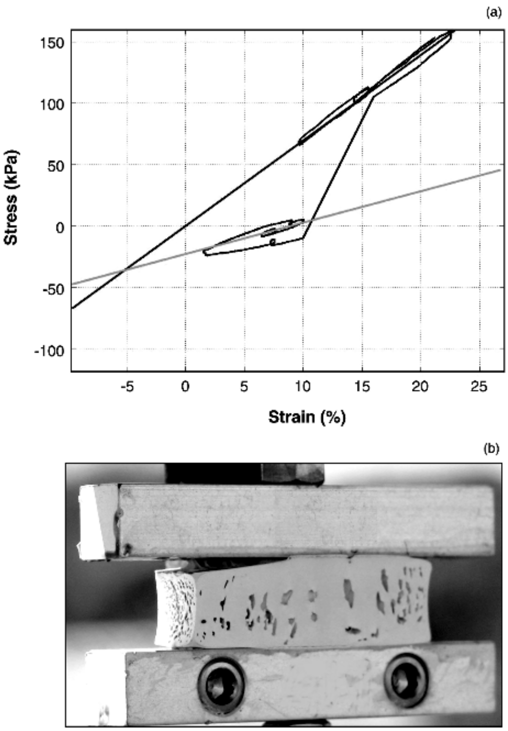

Figure 7—Failure of a sealant specimen: (a) stress-strain plot showing the failure (failure occurred on May 16, 2003, at about 1:15 pm), (b) photograph showing an adhesive failure. Note the failure shows a slope because the two data points were taken 15 min apart.

specimen to stresses similar to that obtained via thermal expansion or contraction of metals, glass, ceramics, or polymers. This apparatus simulates the thermally driven designs previously used, but it is driven primarily by changes in relative humidity and water, not temperature. In CS (*Figure* 4), the test specimens are placed in compression (C) as the wood swells, which subjects the specimens to stresses similar to that obtained when sealants are used on wood. The wood moved against an aluminum frame to produce a cyclic movement. The aluminum was attached to the bar at the top of the apparatus; the load cell and specimen are uni-axial (*Figure* 5). All fasteners in the apparatus were stainless steel. Each specimen could be attached to a linear variable differential transformer (LVDT). However, we found that deflection could be determined using only four LVDTs.

When we began measuring dimensional changes and loads on specimens, we thought we could determine changes in "apparent modulus," adhesive and cohesive failures, and the effect of temperature, strain, and strain rate by analyzing the vast amount of data we obtained. *Figure* 6 shows the stress-strain plot over four days as a specimen was cycled following a period of rain. This particular test apparatus placed the specimen in decreasing tension as the wood dried (*Figure* 3). The diurnal cycles are superimposed on the overall decrease in tensile strain. The best-fit linear slope of stress-strain linear portions or this type of plot

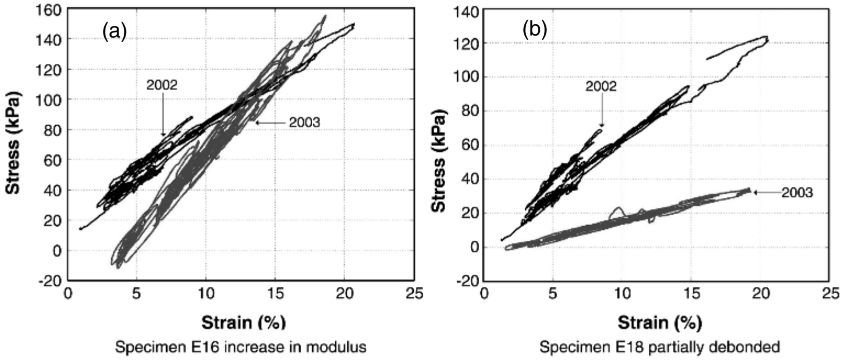

Figure 8—Stress-strain plots for two sealant specimens. Data were collected for three months a year apart. (a) sealant shows an increase in elastic modulus, (b) sealant failed in adhesion.

gives an "apparent elastic modulus" (henceforth referred to as elastic modulus). It is an apparent modulus because we did not take into account the change in cross-sectional area or the effect of cohesive or adhesive failure of specimens as they degraded. Cohesive and adhesive failures were easy to observe, and this was reported earlier (*Figures* 7a and b).[5-7] *Figure* 7a shows several cycles with an abrupt change in the slope of the stress-strain plot. This abrupt change occurred at 1:15 pm on May 16, 2003, following a day of rain that placed the specimen close to 25% strain. *Figure* 7b shows the failed specimen. General trends could be determined by comparing plots over time (*Figure* 8). The data could also be plotted to show the modulus versus net cumulative strain energy (*Figure* 9) or cumulative UV radiation (*Figure* 10). Determining modulus in real time proved to be much more difficult because it required selecting data on an equivalent basis of temperature, RH, and strain and calculating modulus from the relatively small number of data points that were taken under similar environmental conditions. Analysis of more than three years of data from previous work[5-7] measuring load-deflection response showed no two times when the temperature, strain, and strain rates on the specimens were the same. During three years, the weather never repeated itself, so the specimens were never at the same condition more than one time in three years. The data were too variable to detect

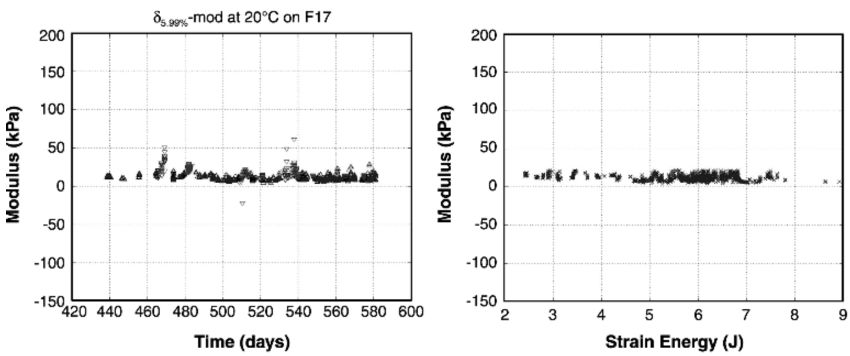

Figure 9—Elastic modulus versus cumulative strain energy and versus time.

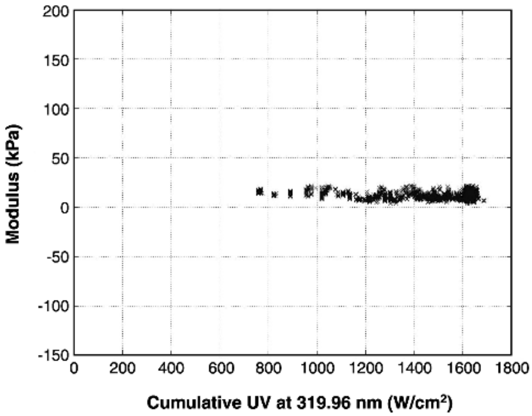

Figure 10—Elastic modulus versus cumulative UV radiation dose at 320 nm.

modulus changes with adequate certainty. We were aware that data scatter could result from the sealant's sensitivity to strain history. This shortcoming of the original uncontrolled cyclic fatigue experiments led to the development of a computer-controlled test apparatus (CCTA).[47] The CCTA made it possible to conduct controlled measurements at the beginning of the exposure to determine specimen quality and properties at various temperatures, strains, and strain rates as the specimens aged. Greater control of the experiment enabled us to discover material properties that were obscured in previous work. The CCTA is capable of temporarily suspending routine exposure testing and performing a precisely controlled stress-strain test (henceforth referred to as "standard strain test") to measure elastic modulus.

EXPERIMENTAL

Weather Station, Test Apparatus, and Data Acquisition

The Forest Products Laboratory field site, which is 5 km west of Madison, WI, has been fully instrumented to collect weather data during outdoor exposure of materials. The weather station, test apparatus, and data acquisition system have been described in detail in previous publications.[5-7,47] We measured temperature wind velocity, relative humidity, rainfall, and UV irradiance at 18 different wavelengths in the range of 290 to 324 nm. The intensity at each wavelength can be integrated to get dose. The dose for other weather factors can also be calculated from the data (total rainfall, degree days, time at dew point). This work involves detailed laboratory and field studies designed to develop SLP methods for sealants. The data from our studies show a clear link between the materials response during weathering and the weather conditions

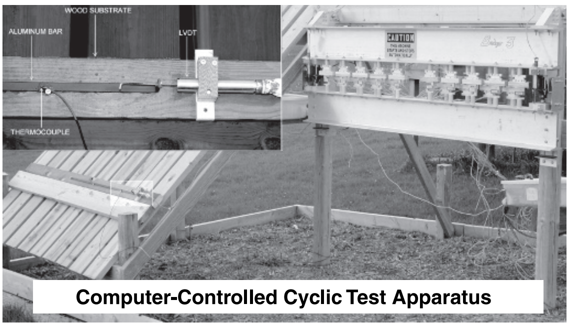

Figure 11—Computer-controlled test apparatus (CCTA) with 18 sealant specimens and load cells mounted. Inset: Close-up of aluminum bar and linear variable differential transformer that provides input to the CCTA.

causing this response. The cyclic fatigue is caused by the changes in weather, and the load and deflection of each specimen is recorded along with all weather data. Data is collected every five minutes.

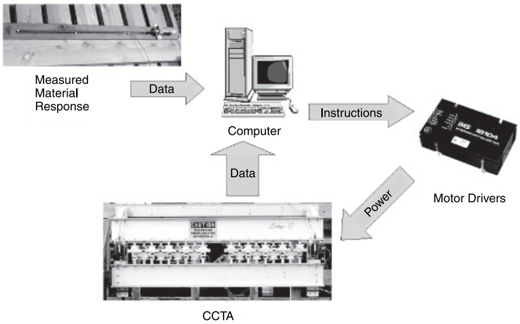

Figure 12—Schematic showing (clockwise) the aluminum bar to obtain temperature-driven dimensional change, computer to modify the dimensional change to meet test objectives, motor driver to control the stepper-motors in test apparatus, the test apparatus, and the feed-back loop to ensure that the movement is correct.

Sealant specimens were mounted on a CCTA capable of holding up to 20 specimens (*Figure* 11). Cyclic motion was obtained from thermally induced changes in dimension of an aluminum bar painted black (*Figure* 12). As the bar changed length, the measurement was fed to a computer. The computer multiplied the measured dimensional changes to meet the target deflections on the specimens. Limits were placed on the maximum movement to ensure the strains did not exceed ±25%. The modified signal drove linear actuators (stepper motors with jack screws) on the apparatus to move one of the two parallel beams, thus applying a deflection to the specimens (*Figure* 13). A feedback loop to the computer ensured that the deflection on the specimen was correct. That is, if the linear actuator failed to apply the proper deflection, the feedback loop corrected this discrepancy. The load on each specimen was measured and the deflection was either measured directly or calculated from the measured movement of the apparatus (*Figure* 14).

All specimens were subjected to a standard strain test every 4 h during the exposure to determine changes in modulus caused by temperature, RH, strain history, and degradation. The standard strain test was used to determine the elastic modulus of specimens by imposing a specific strain profile and measuring the resulting stress (*Figure* 15). Each standard strain test consisted of first bringing all specimens to 0 strain for 60 s, then imposing the strain profile consisting of a constant rate ramp up to 10% tensile strain, a 60-s hold, a constant rate ramp down to 10% compressive strain, a 60-s hold, and a constant rate ramp back to zero strain. This cycle was repeated to eliminate the Mullins effect (a property of elastomers causing a stiffer modulus measured on the first cycle than on subsequent cycles).

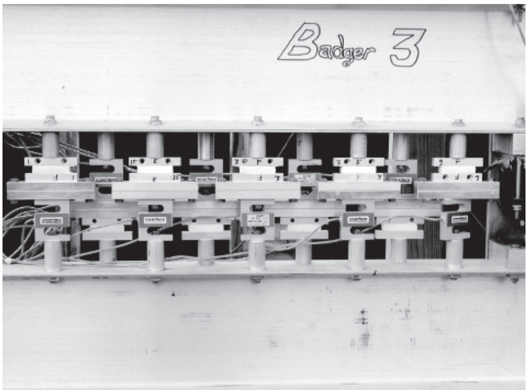

Figure 13—Nine sealant specimens and load cells mounted on the computer-controlled test apparatus.

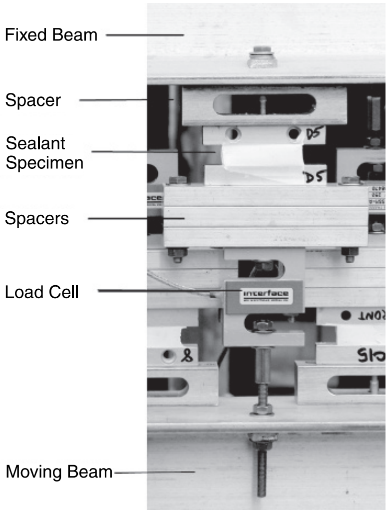

Figure 14—Close-up of a specimen mounted in the test apparatus showing the stationary beam, spacers, sealant specimen, load cell, and the moving beam.

Sealants

Two sealants, one low modulus and one high modulus, were selected from the seven different experimental sealants formulated for these studies. The formulations were designed to have a range of properties because the intent of this research is to establish a protocol for future work. The sealants were selected to give different load deflection characteristics and have short service lives (generally less than three years).[5-7] For the study reported here, six specimens from the A-formulation and seven specimens from the B-formulation were evaluated periodically during two years of outdoor exposure using our standard strain test as described above. The specimens for the two formulations are labelled as A1, A2, A3, A4, A5, and A6, and B1, B2, B3, B4, B5, B6, and B7. Our industry partners prepared the specimens. We did not control their manufacturing nor did we know the specimen formulations. Therefore, we are treating them as distinct experimental units, rather than experimental replicates.

RESULTS AND DISCUSSION

Cyclic Fatigue

To determine chemical changes (additional crosslinking or bond cleavage) in sealants during exposure, we attempted to measure changes of physical properties as they age. We chose this approach to avoid the difficulty of directly measuring chemical changes in situ during exposure. We measured elastic modulus. Specimen degradation, whether crosslinking or bond cleavage, could be expressed as a change in modulus of the specimens. As specimens continue to crosslink, we expected the modulus to increase; conversely, as bonds cleaved the specimen modulus should decrease. If both crosslinking and bond cleavage occur, it would be difficult to determine these changes by measuring the changes in modulus. In addition, other factors such as stress relaxation, strain hard-

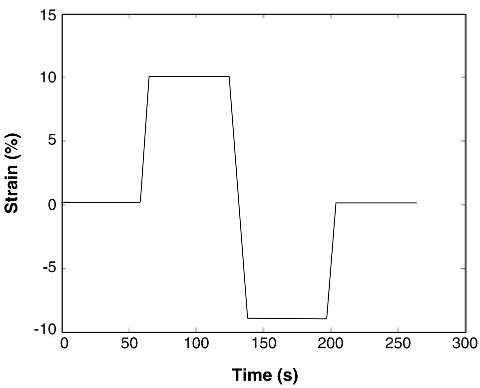

Figure 15—An example of the strain versus time profile imposed on specimens during the standard strain test.

ening, and Mullins effect could affect our measurements. As we did not know the chemistry, the measurement of modulus was the first attempt to quantify possible chemical changes in situ during the test. Scatter in the measurement data could also obscure changes in modulus; therefore, all other sources of experimental variability must be identified and accounted for. Possible sources of variability include, but are not limited to, temperature, water content, and strain history of the specimens as well as imposed strain rate, measurement errors, and electronic noise.

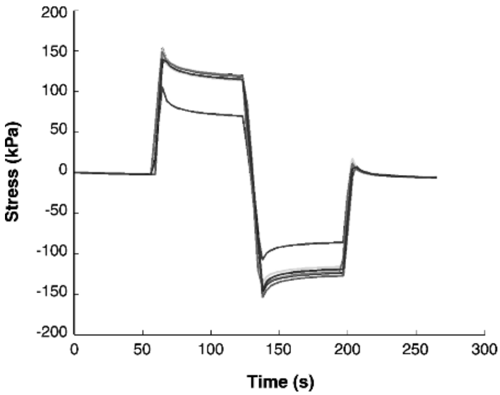

Figure 16—Stress response versus time of B-formulation specimens to the standard test strain profile. Test was performed at the beginning of outdoor exposure.

Temperature, water content, relative humidity, and strain history of the specimens were controlled by environmental conditions and varied with the weather. Temperature, relative humidity, and strain history were measured and recorded. Currently, there are no means of measuring water content, though it is believed to depend on relative humidity and strain history. We minimized measurement and signal errors by selecting force transducers sensitive to ±1.25 N (0.3 lb) and LVDTs sensitive to ±0.2 mm (0.0007 in.), shielding all signal cables, and calibrating all instrumentation. We decreased experimental error by holding controllable factors such as short-term strain history and strain rate constant. The standard strain test always used the same strain rate. We measured initial modulus on all specimens prior to exposure to determine specimen-to-specimen variation.

The strain versus time profile of the standard strain test is shown in *Figure* 15 and stress response versus time for seven B-formulation specimens measured at the beginning of the exposure is shown in *Figure* 16. The plots for most of the specimens overlap considerably, but one is much different. This was our first indication of considerable variability among the industry-prepared specimens within each formulation group. Data from these two time series (stress versus time and strain versus time) were combined to create a stress versus strain plot for each specimen for every test (e.g., spec-

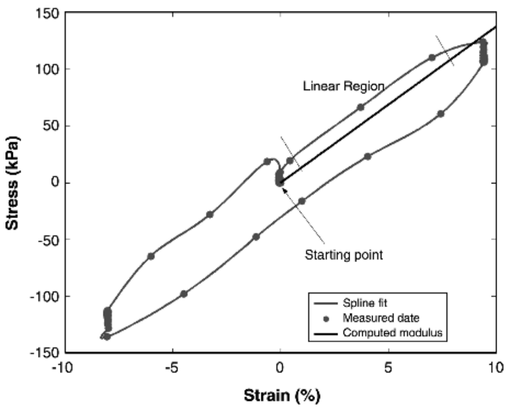

Figure 17—Stress versus strain for sealant specimen B7 for a standard test showing linear portion of the curve used in calculating the apparent elastic modulus. The line is a computed best-fit estimate of the slope.

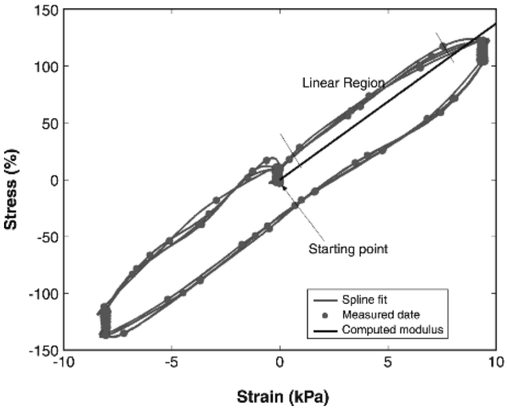

Figure 18—Stress versus strain for sealant specimen B7 showing four consecutive standard tests. The first curve shows a slightly higher maximum stress, whereas the next three curves are similar to each other. The line is a computed best-fit estimate of the slope.

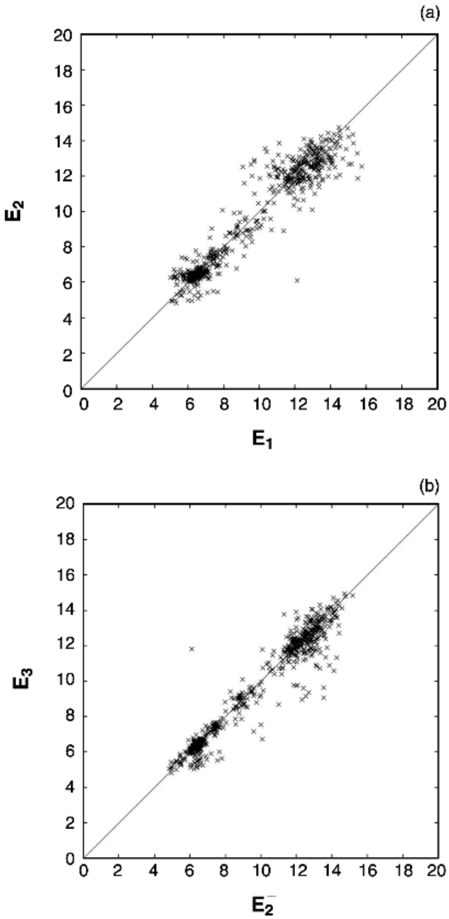

Figure 19—Apparent elastic modulus calculated from (a) second standard test versus first standard test, (b) third standard test versus second standard test. Data points indicating perfect experimental replication lie along a line having slope equal 1. Plot b shows a tighter grouping than plot a (especially in the higher modulus B specimens), indicating better replication.

imen B7, *Figure* 17). This plot shows a fairly constant slope during the initial tension phase of the standard test. A linear regression of this portion of the stress versus strain plot was used to compute the apparent elastic modulus. Similar analyses were completed for all specimens, and elastic moduli calculated from these standard tests were less variable than those calculated from linear portions of weather-induced stress-strain data obtained in previous studies.[5-7] Three problems were encountered in analyzing the data from these uncontrolled tests. We could not control the initial strain, the strain rate, or account for the Mullins Effect. We had no control over the previous stress-stress-cycles, therefore dissimilar strain histories gave variable and often misleading measurements.

Mullins Effect is well known to occur with viscoelastic materials such as sealants and was previously shown to occur with these particular sealants.[48,49] We characterized the Mullins Effect on the standard strain test by conducting four successive standard tests (*Figure* 18). The moduli extracted from the linear portions of the plots were different for successive tests. Plots of the modulus of the second test versus the modulus of the first test (E2 versus E1) and third test versus second test (E3 versus E2) were used to show these differences (*Figures* 19a and 19b). Points that fall on the diagonal line indicate exact replication. If there were no measurement errors in these experiments, points above the line would indicate stiffening and those below the line would indicate softening of the specimens in the subsequent test. Comparison of the plots in *Figures* 19a and 19b show a clear shift of data to below the line, indicating softening of specimens between tests, which is what would be expected from the Mullins Effect.[48,49] The points above the line are clustered close to the diagonal line and we attribute the points above the line to experimental error. There may be other factors that could be responsible for the points above the line, such as compressive set in the specimens prior to the test. Additional studies are under way to investigate this and other possible causes for this apparent variation. Histograms of this comparison show slightly decreased scatter in the data (*Figure* 20). The observed change between the second through the fourth test was small; therefore, we are confident that two cycles were sufficient to minimize the Mullins effect in our data.

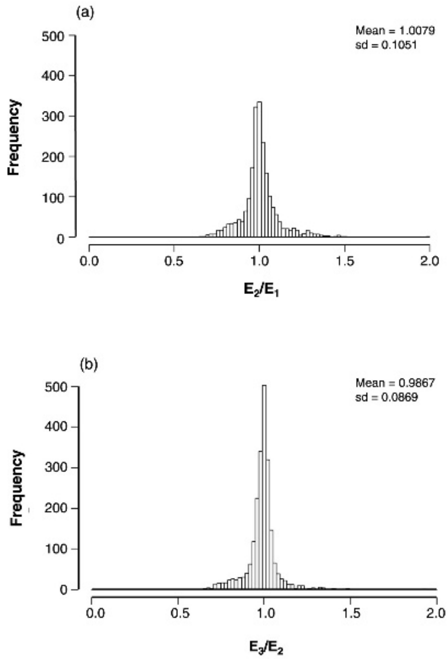

Figure 20—Histograms of (a) E2/E1 and (b) E3/E2. A value of 1.0 indicates perfect experimental replication. As in Figure 10, the data indicate that tests 2 and 3 are better replicates than tests 1 and 2.

As we developed test methods that took into account the Mullins Effect, considerable differences became apparent among the specimens within the same formulations. The standard strain test performed shortly after the specimens were placed in test showed distinct differences among the specimens. As mentioned previously, the plot of the B specimens (*Figure* 16) clearly shows that one of the specimens is different. We have no explanation for this, but it indicates that we may have considerable specimen-to-specimen variability. This high variability in the specimens may make it difficult to average the data for each formulation to calculate a material property such as modulus. To determine if specimens were statistically distinct, we performed an analysis of variance (ANOVA), and plotted confidence intervals for all pair-wise differences between specimens. The A specimen contrasts are seen in *Figure* 21a, and the B specimen contrasts are seen in *Figure* 21b. The horizontal lines show a 95% confidence interval for the difference between each pair of specimens. If that line crosses the dotted vertical line toward the left of the plot (difference = 0), then those specimens are not significantly different. The 95% confidence limits were computed taking into account the number of comparisons performed, so the 95% refers to a family-wise error rate, not a test-wise error rate. Among the A-formulation specimens, A1 and A3 are not distinct. All other A specimens are distinct. Among B-formulation specimens, B2 and B5 are not distinct. All other B specimens are distinct. Box and whisker plots show the variability in the data for the A and B specimens (*Figures* 22a and 22b). Outliers are marked with a circle (determination of outliers was done automatically by the R statistical software). The whiskers extend the full range of the non-outlier data. The box extends from the 25th to the 75th percentile of the non-outlier data. The thick line indicates the mean.

The ANOVA suggests that all our specimens are statistically distinct. We did not have control over the preparation of the specimens; our industry partners provided them. For this reason, we did not feel it was appropriate to pool data from multiple specimens in our analysis. If they are not experimental replicates, and we cannot say with certainty that they are, then conclusions from pooled

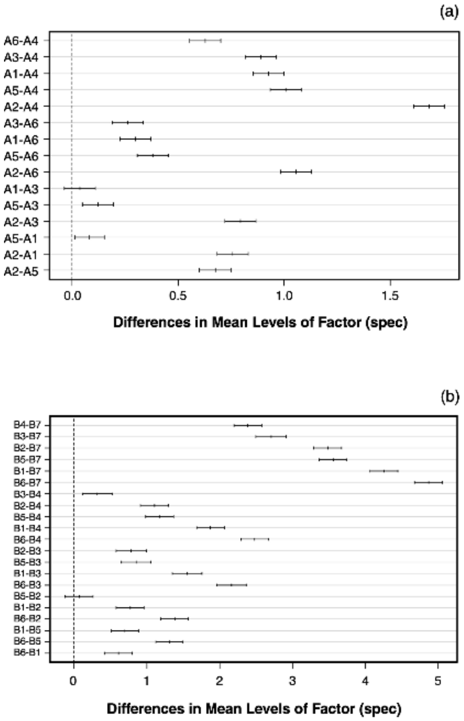

Figure 21—Results of multiple comparison test used to determine whether individual specimens are statistically different from each other. Horizontal bars indicate 95% confidence intervals of the difference between pairs of specimens. A difference of zero (dashed line) indicates 95% confidence that two specimens have the same apparent elastic modulus. (a) depicts A-formulation specimens, (b) depicts B-formulation specimens.

analysis could be misleading. From this point on in the discussion, all analyses are for individual specimen.

Temperature and relative humidity (RH) are important environmental factors for these specimens. Therefore, we sorted the data on the basis of these factors and created “bins” containing data that fall within a specified range of conditions (measurements taken at similar temperature and RH). *Table* 1 shows the number of data points within each bin for specimen B7. Taking the data from the fullest bin and plotting it versus time (*Figure* 23), there is little we can conclude. Two periods, roughly six months apart, have the same conditions. Within each period, the data has considerable scatter. To draw any meaningful conclusions from this data, we will use statistical techniques.

Statistical Analysis

Statistical analysis was used to show the variability in the specimens and to determine the relationship between weathering stressors and material degradation. Specifically, we attempted to detect changes in elastic modulus as the specimens were exposed outdoors. The difficulty lies in separating changes in modulus caused by material degradation from variation in modulus caused by environmental conditions. The weather did not repeat itself, but the CCTA provided the capability to repeat standard tests—thus eliminating initial strain, strain rate, and Mullins Effect as variables. The binning of data according to specific temperature and relative humidity ranges gave sufficient data to construct a model to explain these effects on modulus over the range of weather conditions observed during the exposure. The model also includes factors for energy inputs into each specimen from UV radiation and cumulative strain. The simplest model to characterize these sealants uses a linear combination of these independent environmental factors. We recognize that there are interactions among the factors, particularly temperature and RH; however, this model gives a starting point. Future work will need to

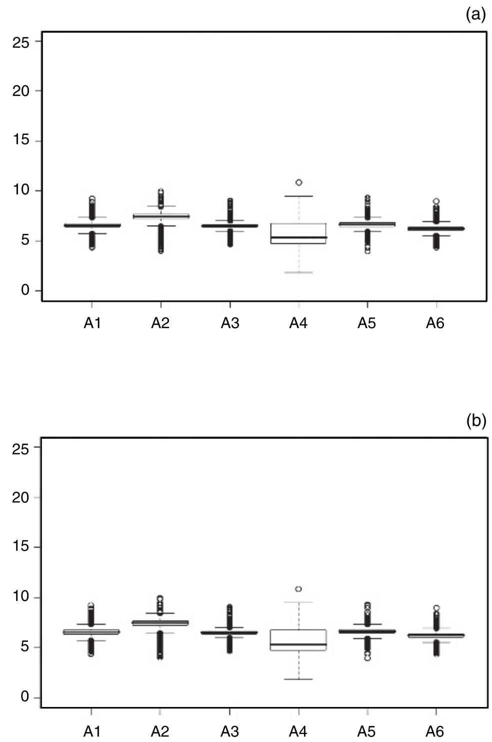

Figure 22—Box and whisker plots of apparent elastic modulus for all data. (a) A–formulation specimens and (b) B–formulation specimens. The heavy horizontal lines indicate average modulus, the rectangular boxes enclose values falling between the 25th and 75th percentiles and the whiskers indicate the range of the data excluding outliers. Outliers are depicted as circles.

Table 1—Number of Standard Tests Binned by Environmental Factors (Specimen B7). Entries with 10 or More Data Points Are Displayed in Bold

Temperature (°C) \ RH (%)	35	40	45	50	55	60	65	70	75	80	85	90	95	100
-10														
-7.5							1		5	5	1	5	1	5
-5							2	2	5	7	4	9	5	**11**
-2.5						2	3	4	3	7	9	**10**	**17**	**10**
0					3	7	6	1	**13**	**18**	**13**	**15**	**21**	**34**
2.5				2	3	6	3	5	**14**	6	9	8	9	**21**
5		1	1	4	7	4	5	**12**	6	6	**14**	9	**19**	**51**
7.5				1	3	3	1	1	2	4	4	3	6	**19**
10	3	4	3	**11**	9	6	5	7	4	3	**17**	**14**	4	**17**
12.5		2		2			3	5	4	3	2	5	2	**16**
15		1	4	3	4	7	6	3	4	5	3	4	7	**39**
17.5	1		3	4	1	5	3	2	4	8	6	9	9	**29**
20		1	3	3	3	5	1	1	7	7	5	**13**	**17**	**26**
22.5	1	3	1		2	2	5	5	9	**14**	**12**	4	6	**38**
25	1		3	4	6	**10**	9	**10**	9	**11**	5	**11**	8	**15**
27.5			4	2	3	8	**10**	3	7	2	7	4	2	2
30			3		2	4	6	4	7	4	2	2		
32.5				1		2	3	3	2					
35					1	1	1							

be directed toward developing an understanding of other environmental factors causing degradation and the non-linear response of these materials to those factors.

Other investigators are working on developing constitutive models of elastomers.[50-52] These models have been successful for particular materials tested under laboratory conditions using viscoelastic materials having known chemistries with a limited number of additives. It is difficult to extend these models to describe the behavior of the sealants used in our work because the chemistry of the sealants was not known and the deflection of the specimens varied because of the weather.

Our initial analysis was a multiple linear regression using ordinary least squares to fit the data[53,54]:

sqrt(mod) = b0 + b1*Cold + temp K*(b2+b3*Cold) +
RH*(b4+b5*Cold) + b6*CSE + b7*CUVE +
b8*Time + N(0,MSE)

where

- sqrt(mod) is the square root of the modulus
- b0 through b8 represent the regression coefficients
- temp K denotes the ambient temperature in Kelvins
- Cold is a {0, 1} variable, which will be 1 when the ambient air temperature is less than 273 K
- RH denotes the relative humidity

- CSE denotes cumulative strain energy in joules applied to the specimen; this is a measure of the net physical work done on the specimen through cyclic loading/unloading
- CUVE denotes the cumulative UV energy in joules applied to the specimen
- Time denotes the exposure time in seconds
- N (0, MSE) denotes normally distributed error with a constant variance over the range of the data

The terms for above and below 0°C are included because we have observed a change in modulus at 0°C for many of the sealants being evaluated in this work. This is discussed below.

This model stipulates that the shape of the response surface for these materials is a pair of planes, one above freezing and one below freezing. Stepwise selection was used to reduce these models by removing statistically non-significant terms. Results of this process are summarized for each specimen (*Table* 2). The R^2 values indicate the percentage of the variation in the data that the model explains. The *p*-values indicate how well the model explains that variation (0.05 or lower indicates statistically significant explanatory power). The b0 and b1 terms are intercepts at 0 K. They are required for building the model, but have no physical meaning independent of the model. The b2 term indicates the change in modulus for a 1 K change in temperature when the temperature is above freezing. The sum of b2 and b3 indicate the change in modulus for a 1 K change in temperature when the ambient temperature is below freezing. The b3 term can then be interpreted as the additional effect of temperature below freezing. The b4 term indicates the change in modulus for a 1% change in RH when the ambient temperature is above freezing. The sum of b4 and b5 indicate the change in modulus for a 1% RH change when the ambient temperature is below freezing. The b5 term is the additional effect of RH below freezing. The b6 term indicates the change in modulus caused by cyclic loading. The b7 term indicates the change in modulus caused by UV degradation. The b8 term indicates time-dependent degradation of the specimen.

Calculation of the coefficients (*Table* 2) was straightforward using all the data in all the bins (*Table* 1; approximately 1250 tests) for a particular specimen. Using these coef-

Table 2—Estimated Model Parameters Produced by Multiple Regression. Coefficients That Were Not Significantly Different from Zero Have Been Omitted

	b0	b1 (cold)	b2 (temp)	b3 (cold*temp)	b4 (RH)	b5 (cold*RH)	b6 (CSE)	b7 (CUVE)	b8 (time)	R^2	p
A1	3.35E+00		2.86E-03				-4.49E-03	-2.32E-10	5.94E-09	0.11	<0.0001
A2	3.88E+00	-1.39E-02	4.12E-03				-4.29E-03		1.22E-09	0.36	<0.0001
A3	3.35E+00	8.16E-01	2.75E-03	-3.04E-03			-6.06E-03	-3.13E-10	1.12E-08	0.31	<0.0001
A4	1.42E+00	-2.81E-02			-9.62E-04		-4.56E-03	4.11E-10	1.57E-08	0.67	<0.0001
A5	3.79E+00	-1.48E-02	1.89E-03		-1.70E-04		-6.88E-03	-2.68E-10	1.16E-08	0.28	<0.0001
A6	3.44E+00	4.84E-01	2.31E-03	-1.80E-03			4.01E-03	-1.96E-10	3.75E-09	0.38	<0.0001
B1	5.83E+00	4.05E+00	-1.10E-02	-1.48E-02	-9.52E-04			-7.33E-10	1.15E-08	0.73	<0.0001
B2	7.28E+00	4.06E+00	-1.20E-02	-1.53E-02	-1.35E-03	1.30E-03		-7.02E-11		0.72	<0.0001
B3	6.82E+00	4.40E+00	-8.50E-03	-1.61E-02	-9.36E-04		-7.50E-03	-1.34E-09	4.56E-08	0.75	<0.0001
B4	7.51E+00	3.74E+00	-9.58E-03	-1.37E-02	-8.91E-04		-4.65E-03	-1.37E-09	2.79E-08	0.77	<0.0001
B5	6.12E+00	3.90E+00	-1.14E-02	-1.42E-02	-9.74E-04			-6.46E-10	8.57E-09	0.82	<0.0001
B6	6.31E+00	5.02E+00	-1.23E-02	-1.83E-02	-8.72E-04			-3.96E-10	9.04E-09	0.73	<0.0001
B7	5.41E+00	3.92E+00	-1.19E-02	-1.42E-02	-1.12E-03			-4.89E-10	1.10E-08	0.67	<0.0001

Table 3—Example Calculation of Initial Modulus Using the Model from *Table* 4 on Specimen B7

Coefficients		Terms		Results	
b0	5.41E+00				5.41
b1	3.92E+00	cold	0	b1* cold	0.00
b2	-1.19E-02	temp	278	b2* temp.	-3.31
b3	-1.42E-02	cold-temp	0	b3* (cold*temp)	0.00
b4	-1.12E-03	RH	100	b4*RH	-0.11
b5		cold*RH	0	b5* (cold*RH)	0.00
b6		CSE	0	b6*CSE	0.00
b7	-4.89E-10	CUVE	0	b7*CUVE	0.00
b8	1.10E-08	Time	104032200	b8*Time	1.15
				sqrt(mod)	3.14
				Predicted Modulus 9.84 kPa	
				Measured Modulus was 10.50 kPa	

Note: The value for "time" (104032200) for the b8 corresponds to time in seconds from the beginning of the experiment. The predicted modulus from this calculation is 9.84 kPa and the measured modulus for the first three months of exposure is 10.50 kPa.

ficients, a modulus can be calculated for any specimen. Simply measure the required factors, multiply them by the appropriate b-coefficient, sum the result, then take the square to predict the modulus. An example of this calculation for specimen B7 is presented in *Table* 3. Some of these coefficients can be independently interpreted as rates of change. For example, b8 gives the rate of time-dependent degradation in kPa/s. The two intercept terms (b0, b1) lack physical meaning outside the model. The temperature and RH related terms can be combined to compute above/below-freezing rates of change. For example, b2 gives the rate of change with temperature above freezing in kPa/K and (b2 + b3) gives the same for the below freezing case.

To verify that these models were functioning correctly, we checked the model predictions against the mean modulus computed within a number of bins. The results are seen in *Table* 4. There is a good correspondence between predicted modulus and measured values. Similar correspondence results were obtained for other specimens at various temperatures and RHs. All of the models had significant *p*-values, indicating that the correlation between our data and the model did not arise simply by chance (*Table* 2). The A specimens are not well characterized (R^2 values range between

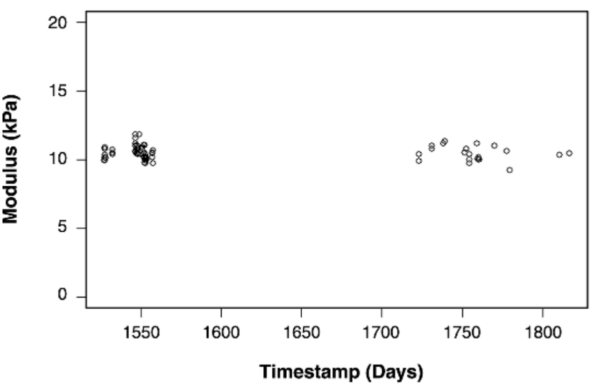

Figure 23—Modulus versus time for specimen B7 selected for 5 ± 1.25°C and 97.5%–100% RH. The 0 on the time axis is the date we brought our weather station on line about five years ago.

Table 4—Comparison of Model Output and Date Mean in Selected Bins for Specimen B7 and Specimen A6

Specimen	Temp (°C)	RH (%)	N	Predicted Modulus (kPa)	Predicted Modulus (kPa)	% Error
A6	–2.5	95	17	6.3	6.24	0.96
A6	0	95	21	6.25	6.22	0.55
A6	0	100	35	6.22	6.26	–0.54
A6	5	95	19	6.32	6.35	–0.54
A6	10	55	10	6.38	6.36	0.3
B7	–2.5	95	17	11.29	11.15	1.26
B7	0	95	21	11.07	11.02	0.48
B7	0	100	35	11.09	11.49	–3.48
B7	5	95	19	10.53	10.58	–0.43
B7	10	55	9	10.31	10.13	1.8

Both the "measured" and the "predicted" refer to whole-exposure averages.

0.11 and 0.38). Among the B specimens, R^2 values range from 0.67 to 0.82. These R^2 values indicate that the B specimens are much better characterized by these models. The Bs appear to be more sensitive to environmental factors than the As.

This modeling effort is meant only as a first pass. We are certain that the true behavior of these materials is non-linear. We are also certain that there are very important non-linear interactions between environmental factors. Unfortunately, we do not yet understand the nature of those relationships well enough to construct a better model than the one we present here. Future effort will focus on improving the accuracy and increasing the complexity of our models. We will work to generalize short-exposure laboratory condition models developed by other investigators such that they can handle environmental variation and incorporate a time-series component. However, note that the simple model could explain as much as 80% of the behavior of the B specimens. Most of the specimens responded to RH, but not all. Many specimens showed a distinct difference in modulus above and below 0°C. *Figure* 24 shows this change in modulus for the B7 specimen.

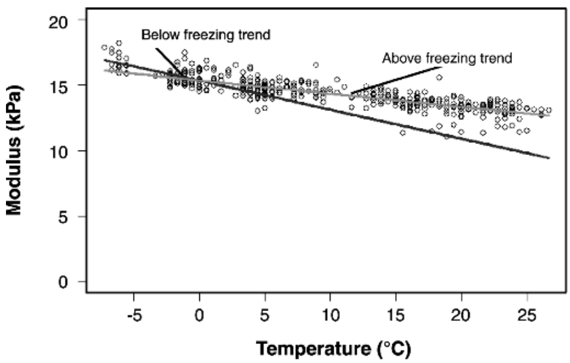

Figure 24—Modulus versus temperature for specimen B7 selected for 97.5%–100% RH, with lines showing predicted values above and below freezing. Note that the best-fit slope is not identical above/below 0°C.

The ability to conduct precise standard tests allowed us to identify experimental anomalies and take steps to correct them or to eliminate the data from the data set. Changes in elastic modulus caused by weathering have been detected and can be partially explained in terms of energy flux into the specimen from cyclic UV exposure and loading/unloading (*Table* 2, columns b6 and b7). There is some residual correlation with exposure time (*Table* 2, column b8) even after strain and UV energy inputs are considered. It is our belief that once a sufficient dose/damage relationship is found, we will be able to eliminate time and account for the degradation in terms of the energy input into the specimens and the environmental factors.

Though improvements have been made in our data analysis, further improvement may be possible by increasing the speed of measurement. The current system has a maximum measurement rate of 5.3 measurements/ specimen/second for 18 specimens in the apparatus. We plan to install a new faster data acquisition and control system. This system has an accurate electronic pulse generator that will improve the timing of step commands to the motors. This will increase the linearity of the standard test strain ramp-up and improve reproducibility of the tests. The new system will be capable of measuring load and displacement hundreds of times per second. Faster measurement means more data points can be taken during the standard strain test and used for calculating modulus. Together, the fast accurate pulse generator and the high data acquisition rate will allow modification of the standard test to incorporate a higher rate of strain ramp-up. Faster strain application decreases the amount of relaxation during a test, resulting in less viscous and more elastic response of the elastomeric specimens. These improvements are expected to decrease variability of the calculated modulus, enabling detection of smaller material changes caused by environmental conditions and weathering.

CONCLUSIONS

We have shown that data collected from the CCTA can be used to develop models to help us to understand the effects of temperature, RH, cyclic fatigue, and UV exposure. Based on these models, we can make statements about the rate of degradation for given doses of UV or cyclic loading. This is a promising first step on the path toward understanding the factors that cause these specimens to age.

We have demonstrated that the response of sealants and the weather-causing cyclic movement can be monitored continuously. From our earlier studies, measurement of load and deflection during this cyclic movement could be used to determine the elastic modulus; however, a controlled standard test using the computer-controlled CCTA gave much better results. The standard strain test made it possible to evaluate specimen quality at the beginning of the test and to determine the variability in a group of replicate specimens. The data from the standard test were used to construct a model to evaluate the effect of temperature and relative humidity on the elastic modulus. As one would expect from these viscoelastic sealant materials, the elastic modulus was dependent on temperature and RH, and we were able to detect changes in modulus as the specimens aged. A plot of elastic modulus versus temperature showed a change in modulus at 0°C, indicating a change in the plasticizing effect of moisture above and below freezing.

ACKNOWLEDGMENTS

We thank Russell Goodrich and Patrick Neale (Smithsonian Environmental Research Center, Edgewater, MD) for their help in setting up, calibrating, and monitoring the UV radiometer; Dave Eustice and Larry Zehner (Forest Products Laboratory) for building the test apparatus; and all the members of the FPL shops for their help with the initial stages of setting up the experiment.

References

(1) White, C.C., Martin, J., Weber, S., Shultz, L., and Williams, R.S., "Reliability-Based Method for Service Life Prediction of Materials," *Proc. SPE/ANTEC National Meeting*, 2002.

(2) White, C.C., Hunston, D.L., and Williams, R.S., "Challenges in Characterizing Sealant," *Proc. ANTEC Conference from Society of Plastics Engineering*, Nashville, TN, 2003.

(3) White, C., Embree, N., Buch, C., and Williams, R.S., "Design, Development, and Testing of a Hybrid in situ Testing Device for Building Joint Sealant," *Rev. Sci. Instrum.*, 76, 045111 (2005).

(4) White, C.C. and Hunston, D.L, "Issues Related to the Mechanical Property Characterization of Sealants," *Durability of Building and Construction Sealants and Adhesives*, ASTM Special Technical Publication 1453, p. 325-334, 2004.

(5) Williams, R.S., Sanandi, A., Halpin, C., and White, C., "Merging Weather Data with Materials Response Data during Outdoor Exposure," *Proc. Third International Woodcoatings Congress*, The Hague, The Netherlands, 2002.

(6) Williams R.S., Lacher, S., Halpin, C., and White, C., "Development of Test Apparatus for Service Life Prediction of Sealant Formulations and Evaluation of Data from 18 Months of Outdoor Weathering," *Proc. Fourth International Woodcoatings Congress*, The Hague, The Netherlands, 2004.

(7) Williams, R.S., Lacher, L., Halpin, C., and White, C., "Evaluating Weather Factors and Material Response during Outdoor Exposure to Determine Accelerated Test Protocols for Predicting Service Life," in *Service Life Prediction: Challenging the Status Quo*, Martin, J.W., Ryntz, R.A., and Dickie, R.A. (Eds.), Federation of Societies for Coatings Technology, Blue Bell, PA, p. 171-185, 2005.

(8) Williams, R.S., Lacher, S., Halpin, C., and White, C., "Evaluation of Materials During Outdoor Testing Using a Computer-Controlled Test Apparatus," *Proc. Fifth International Woodcoatings Congress*, Prague, Czech Republic, 2006.

(9) Martin, J.W. and Bauer, D.R. (Eds.), *Service Life Prediction: Methodology and Metrologies*, American Chemical Society Series 805, Oxford Press, New York, 2001.

(10) D 822 96, Standard Practice of Conducting Tests on Paint and Related Coatings and Materials using Filtered Open-Flame Carbon-Arc Light and Water Exposure Apparatus, *Annual Book of ASTM Standards*, Vol. 04.07, ASTM International, West Conshohocken, PA, 2000.

(11) D 5031 96, Standard Practice of Conducting Tests on Paint and Related Coatings and Materials using Enclosed Carbon-Arc Light and Water Exposure Apparatus, *Annual Book of ASTM Standards*, Vol. 06.01, ASTM International, West Conshohocken, PA, 2001.

(12) G 26 96, Standard Practice for Operating Light-Exposure Apparatus (Xenon-Arc) With and Without Water for Exposure of Nonmetallic Materials, *Annual Book of ASTM Standards*, Vol. 06.01, ASTM International, West Conshohocken, PA, 2001.

(13) G 53 96, Standard Practice for Operating Light- and Water-Exposure Apparatus (Fluorescent UV-Condensing Type) for Exposure of Nonmetallic Materials, *Annual Book of ASTM Standards*, Vol. 06.01, ASTM International, West Conshohocken, PA, 2001.

(14) D 4587 91, Standard Practice of Conducting Tests on Paint and Related Coatings and Materials using a Fluorescent UV-Condensation Light- and Water-Exposure Apparatus, *Annual Book of ASTM Standards*, Vol. 06.01, ASTM International, West Conshohocken, PA, 2001.

(15) Martin, J.W., " A Critical Review of the Role of Field-Exposure Experiments in Predicting the Service Life of Coatings," *Plastics and Coatings Durability, Stabilization, Testing*, Ryntz, R.A. (Ed.), Ch. 2. Hanser Gardner Publications, Inc., Cincinnati, OH, p. 33, 2001.

(16) Martin, J.W., "Repeatability and Repeatability of Field Exposure Results," *Service Life Prediction Methodologies and Metrologies*, Martin, J.W. and Bauer, D.R. (Eds.), ACS Symposium Series 805, American Chemical Society, Oxford Press, NY, p. 1, 2001.

(17) Nguyen, T., Rezig, A., Gu, X., Kidah, B., and Martin, J.W., "Degradation Kinetics and Mechanisms of Aliphatic Amine-Cured Epoxy Coatings Exposed to Xenon Arc UV and Outdoors," *Proc. Western Coatings Conference*, Las Vegas, NV, 2005.
(18) C 1442 99, Standard Practice for Conducting Tests on Sealants using Artificial Weathering Apparatus, *Annual Book of ASTM Standards*, Vol. 04.07, ASTM International, West Conshohocken, PA, 2000.
(19) C 718 93, Standard Test Method for Ultraviolet (UV)-Cold Box Exposure of One-Part, Elastomeric, Solvent-Release Type Sealants, *Annual Book of ASTM Standards*, Vol. 04.07, ASTM International, West Conshohocken, PA, 2000.
(20) C 732 95, Standard Test Method for Aging Effects of Artificial Weathering on Latex Sealants, *Annual Book of ASTM Standards*, Vol. 04.07, ASTM International, West Conshohocken, PA, 2000.
(21) C 734 93, Standard Test Method for Low-Temperature Flexibility of Latex Sealants After Artificial Weathering, *Annual Book of ASTM Standards*, Vol. 04.07, ASTM International, West Conshohocken, PA, 2000.
(22) C 793 97, Standard Test Method for Effects of Accelerated Weathering on Elastomeric Joint Sealants, *Annual Book of ASTM Standards*, Vol. 04.07, ASTM International, West Conshohocken, PA, 2000.
(23) C 1257 94, Standard Test Method for Accelerated Weathering of Solvent-Release-Type Sealants, *Annual Book of ASTM Standards*, Vol. 04.07, ASTM International, West Conshohocken, PA, 2000.
(24) D 2249 94, Standard Test Method for Predicting Effect of Weathering on Face Glazing and Bedding Compounds on Metal Sash, *Annual Book of ASTM Standards*, Vol. 04.07, ASTM International, West Conshohocken, PA, 2000.
(25) ASTM C 719 93, Standard Test Method for Adhesion and Cohesion of Elastomeric Joint Sealants Under Cyclic Movement (Hockman Cycle), 2005.
(26) Onuoha, U.O., "Durability of One-Part Polyurethane and Polyurethane Hybrid Sealants," *Durability of Building Sealants*, Wolf, A.T. (Ed.), RILEM Pub., France, p. 235–251, 1999.
(27) Brown, N.G., "Assessment of Joint Sealant by Outdoor Exposure in Cyclic Movement Testers," Report No. 01.1-2, CSIRO Division of Building Research, Highett, Victoria, Australia, p. 16-22, 1965.
(28) Burstrom, P.G., "Durability and Ageing of Sealants," In *Durability of Building Materials and Components*, ASTM STP 691, Sereda, P.J. and Litvan, G.G. (Eds.), ASTM Pub., Philadelphia, PA, p. 643–657, 1980.
(29) Karpati, K.K., Solvason, M.R., and Sereda,, P.J., "Weathering Rack for Sealants," *J. Coat. Technol.*, 49, No. 626, p. 44–47 (1977).
(30) Karpati, K.K., "Device for Weathering Sealants Undergoing Cyclic Movements," *J. Coat. Technol.*, 50, No. 641, p. 27–30 (1978).
(31) Lacasse, M.A., "Advances in Test Methods to Assess the Long Term Performance of Sealants," *Science and Technology of Building Seals, Sealants, Glazing and Waterproofing*, Myers, J.C. (Ed.), Vol. III, ASTM STP 1254, ASTM International, Philadelphia, PA, 1994.
(32) Lacasse, M.A., Giffin, G.B., and Margeson, J.C., "Evaluation of Cyclic Fatigue as a Means of Assessing the Performance of Construction Joint Sealants," ASTM Special Technical Publication, n, 1271, *Science and Technology of Building Seals, Sealants, Glazing, and Waterproofing*, ASTM International, Philadelphia, PA, 1996; *Proc. 5th Symposium on the Science and Technology of Building Seals, Sealants, Glazing, and Waterproofing*, Phoenix, AZ, Vol. 5, p, 266-281, 1995.
(33) Lacasse, M.A., Giffin, G.B., and Margeson, J.C., "Laboratory Cyclic Fatigue Test of Silicone Sealant Mini-Specimens,"ASTM Special Technical Publication, n. 1334, *Proc. 7th Symposium on the Science and Technology of Building Seals, Sealants, Glazing, and Waterproofing*, San Diego, CA, p. 51-65, 1998.
(34) Lacasse, M.A. and Margeson, J.C., "Movement during Cure of Latex Building Joint Sealants," *Proc. 6th Annual Symposium on the Science and Technology of Building Seals, Sealants, Glazing, and Waterproofing*, Fort Lauderdale, FL, Vol. 6, p. 129–145, 1999.
(35) Bolte, H., Boettger, T., and Wolf, A.T., "Preliminary Report on the Ageing Behavior of Sealants Exposed to Dynamic Natural and Artificial Weathering," *RILEM Proceedings PRO 10 Durability of Building and Construction Sealants*, p. 151–172, 2000.
(36) Liu, X-X, and Wang, S.T., "Joint Sealant Fatigue Property of Airport Concrete Pavement," *J. Traffic Transport. Engineering*, 6 (1), 44–47 (2006).
(37) Al-Qadi, I.L., Abo-Qudais, S., and Khuri, R.E., "Method to Evaluate Rigid-Pavement Joint Sealant under Cyclic Shear and Constant Horizontal Deflection," *Transport. Res. Rec.*, 1680, p. 30–35 (1999).

(38) Al-Qadi, I.L., and Abo-Qudais, S., ASTM Special Technical Publication, n. 1254, pt 3; *Proc. 3rd Symposium on the Science and Technology of Building Seals and Sealants*, Fort Myers, FL, p. 85–94, 1993.
(39) Miyauchi, H., Enomoto, N., Sugiyama, S., and Tanaka, K., "Artificial Weathering and Cyclic Movement Test Results Based on the RILEM TC 139-DBS Durability Test Method for Construction Sealants," ASTM Special Technical Publication, n 1453, *Durability of Building and Construction Sealants and Adhesives*, American Society for Testing and Materials, West Conshohocken, PA, p. 206–212, 2004.
(40) Sharman, W.R., Fry, J.I., and Whitney, R.S., "Six Years Natural Weathering of Sealants," *Durability of Building Materials*, 2 (1), 79-90 (1983).
(41) Koike, M., Tanaka, K., and Oda, S-I., "Dynamic Properties of Polysulfide and Silicone Sealants in Cyclic Tests of Longer Periods," Report of the Research Laboratory of Engineering Materials, Tokyo Institute of Technology, 7, 159-165 (1982).
(42) Marechal, J.C., and Kalifa, P., "The Prediction of Long-Term Sealant Performance from Dynamic Accelerated Weathering," *Durability of Building Materials and Components 7, Proc. International Conference on Durability of Building Materials and Components*, 7th, Stockholm, p. 54–64, 1996.
(43) Beech, J.C., "Test Methods for the Movement Capability of Building Sealants: The State of the Art, *Materials and Structures*, 18 (108), 473–482 (1985).
(44) Wolf, A.T., "Aging Resistance of Building and Construction Sealants, Part 1," *RILEM Proc. Durability of Building Sealants*, p. 63–89 (1996).
(45) Wolf, A.T., "Attempts at Correlating Accelerated Laboratory and Natural Outdoor Ageing Results," *Durability of Building Sealants*, Wolf, A.T. (Ed.), RILEM Pub., France. p. 181–201, 1999.
(46) Wolf, A.T. and Seneffe, B., "Development of RILEM Durability Test Methods for Curtainwall Sealants," *Proc. International Conference on Durability of Building Materials and Components*, 9, Brisbane, Australia, p. 105/1-105/9, 2002.
(47) Lacher, S., Williams, R.S., Halpin C., and White C., "Development of a Powered Outdoor Sealant Fatigue Test Apparatus," In: *Service Life Prediction, Challenging the Status Quo*, Martin, J.W., Ryntz, R.A., and Dickie, R.A. (Eds.), Federation of Societies for Coatings Technology, Blue Bell, PA, p. 207–216, 2005.
(48) Hunston, D.L., White, C.C., and Williams, R.S., "Viscoelastic Characterization of Sealant Materials," *Proc. 26th Annual Meeting Adhesion Society*, Myrtle Beach, SC, 2003.
(49) Hunston, D.L., White, C.C., and Williams R.S., "Mechanical Behavior of Caulks and Sealants," *Proc. 225th ACS National Meeting*, New Orleans, LA, 2003.
(50) Abraham, F., Alshuth, T., Jerrams, S., "The Dependence on Mean Stress and Stress Amplitude of the Fatigue Life of Elastomers," Deutsches Institut fur Kautschuktechnologie e. V. Publikation, 134, 2001.
(51) Bergström, J.S. and Boyce, M.C., "Time-Dependence of Elastomeric Materials: Experiments and Modeling," *10th International Conference on Deformation, Yield and Fracture of Polymers*, Cambridge, UK, April 1997.
(52) Bergström, J.S., "Constitutive Modeling of Elastomers—Accuracy of Predictions and Numerical Efficiency," PolymerFEM.com, 2005.
(53) Wilkinson, G.N. and Rogers, C.E., "Symbolic Descriptions of Factorial Models for Analysis of Variance," *Applied Statistics,* 22:392-9 (1973).
(54) Chambers, J.M., "Linear Models," Chapter 4 of *Statistical Models in S*, Chambers, J.M. and Hastie, T.J. (Eds.), Wadsworth & Brooks/Cole, 1992.

In: Martin, Jonathan W.; Ryntz, Rose A.; Chin, Joannie; Dickie, Ray A.; eds. Service live prediction of polymeric materials global perspectives. New York, NY: Springer: Chapter 9: pp. 129-151_ 2009